The Number of Discernible Object Colors is Unknown

Kenichiro Masaoka [1,2], *Roy S. Berns* [2], *Mark D. Fairchild* [2], *Farhad Moghareh Abed* [2]
[1]*NHK Science & Technology Research Laboratories, Tokyo, Japan.*
[2]*Munsell Color Science Laboratory, Chester F. Carlson Center for Imaging Science, Rochester Institute of Technology, Rochester, NY, USA.*

Abstract

The number of discernible object colors is estimated over a wide range of color temperatures and illuminance levels using several chromatic adaptation models, color spaces, and color difference limens. Through comprehensive simulation, it is found that there are some limitations to current color appearance models for estimating the number of discernible colors. The fundamental problem lies in the von Kries-type chromatic adaptation transforms that indifferently affect the ranking of the number of discernible colors at different color temperatures.

Introduction

The number of discernible object colors is informative not only because of scientific interest in human color vision, but also because of its potential use in industrial applications such as the development of pigments and dyes, evaluation of the gamut coverage of displays, and design of the spectral power distribution of light sources. The color gamut of imaging media and its main controlling factor, the viewing conditions, are of significant practical and theoretical importance in the reproduction of color images [1]. However, widely varying estimates of the number of discernible colors have been made in the past 100 years [2]. This motivated us to clarify the source of the variation.

Recent estimations have been made using optimal colors. An optimal color is the non-fluorescent object color with the maximum saturation under a given light. Ostwald [3] empirically found that optimal-color reflectances are either 0 or 1 at all wavelengths with at most two transitions. The first mathematical proof of this, which used the convexity of the spectrum locus, is attributed to Schrödinger [4]. MacAdam generated a geometric proof of the optimal color theorem using the CIE xy chromaticity diagram [5] and calculated the chromaticity coordinates of the optimal color loci under illuminants A and C with luminous reflectance Y for the third dimension [6]. The number of discernible colors contained in a three-dimensional solid has been estimated using different perceptual color spaces. In 1998, Pointer and Attridge [7] counted the unit cubes within an optimal color solid under illuminant D65 in the CIE 1976 (L^*, a^*, b^*) color space (CIELAB), estimating some 2.28 million. In 2007, Wen [8] sliced an optimal color solid under illuminant D65 at each lightness unit and chopped each slice into pieces having the unit chroma and the hue differences described in CIE94, obtaining a count of just 352,263. Also in 2007, Martínes-Verdú *et al*. [9] counted the unit cubes packed in optimal color solids under several standard illuminants (A, C, D65, E, F2, F7, F11) and high-pressure sodium lamps in the lightness and colorfulness space (J, a_M, b_M) of the CIECAM02 color appearance model [10]. They assumed this to be the most uniform color space on the basis of their observation that the calculated optimal color solids in the CIECAM02 color space were relatively spherical compared to those in the CIELAB color space and others. They estimated that there were 2.050 million distinguishable colors under illuminant E, 2.046 million under illuminant C, 2.013 million under illuminant D65, 1.968 million under illuminant F7, 1.753 million under illuminant A, and fewer colors under the other light sources. In 2012, Morovic *et al*. [11] calculated optimal color solids in the lightness and chroma space (J, a_C, b_C) of CIECAM02, and estimated a total of 3.8 million colors under illuminant D50, 4.2 million under illuminant F11, and 3.5 million under illuminant A. On the other hand, Morovic *et al.* also pointed out that the currently available models failed to give predictions when extrapolating the psychophysical data they are based on; finally, they made an alternative, safe estimate of at least 1.7 million colors, which was their estimate of the color gamut volume of the LUTCHI data used to build CIECAM02.

In this paper, we provide estimates of the number of discernible colors within the optimal color solid for a wide range of color temperatures and illuminance levels, using a fast, accurate model for computing the optimal colors. Several chromatic adaptation models, color spaces, and limens of color differences are used to clarify the source of the previous, inconsistent estimates.

Method

To verify the previous estimates of the number of discernible colors, we computed the optimal color loci at regular lightness unit intervals of L^* in CIELAB, J in CIECAM02, and J' in a CIECAM02-based uniform color space (CAM02-UCS) [12]. Figure 1 shows a flowchart of the method used to compute an optimal color with a specified central wavelength under an illuminant having a given spectral power distribution and adaptation illuminance level. Optimal colors were searched iteratively so that their lightness values were equalized to the given lightness values. Three different chromatic adaptation transformations were embedded in front of CIELAB with a D65 reference white point. Blackbody radiators at color temperatures ranging from 2,000–4,000 K and standard daylight illuminants at correlated color temperatures (CCTs) ranging from 4,000–10,000 K at 500 K intervals, were used as light sources in the simulation. Illuminance levels of 200 lx (museum standard), 1,000 lx (reference viewing condition), 10,000 lx (outside on cloudy days), and 100,000 lx (outside on sunny days) were considered for the reference white in CIECAM02. Additionally, illuminant E and illuminant series F (F1–F12) were used at an illuminance of 1,571 lx to verify the results of Martínes-Verdú *et al*. [9].
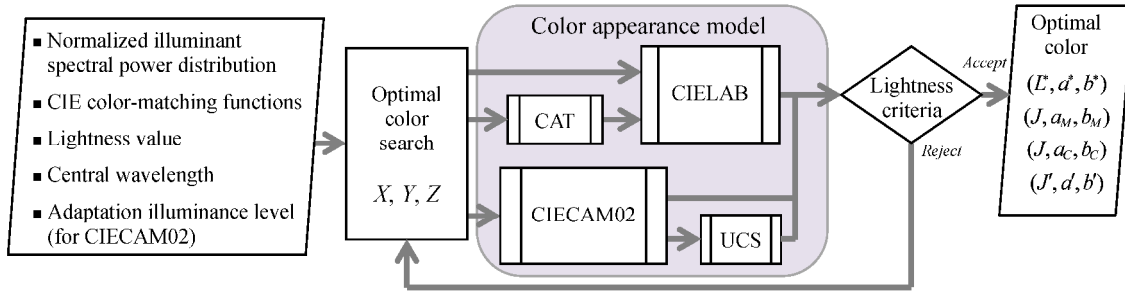
Figure 1. Flowchart for the computation of an optimal color

Optimal color computation

Optimal colors are generated using stimuli with either 0 reflectance (transmittance) at both ends of the visible spectrum and 1 in the middle (Type 1), or 1 at the ends and 0 in the middle (Type 2). Figure 2 illustrates both types, where $\lambda_{\text{cut-on}}$ and $\lambda_{\text{cut-off}}$ represent the cut-on and cut-off wavelengths, respectively. In our simulation, the end-colors (high-pass and low-pass) are handled as Type 1, with the wavelength of transition ($\lambda_{\text{cut-on}}$ or $\lambda_{\text{cut-off}}$) being the end point of the visible spectrum.

A modified version of Masaoka's model [13] was used to calculate the tristimulus values of optimal colors. We used the CIE 1931 color-matching functions $\bar{x}$, $\bar{y}$, and $\bar{z}$ at wavelengths ranging from 400 nm to 700 nm at 1 nm intervals. The spectra of the daylight illuminants were calculated using the CIE equation [14]. Spline interpolation was used for obtaining the CIE color-matching functions and daylight illuminant spectra in order to ensure an adequately small wavelength step of 0.1 nm. The blackbody radiation was calculated using Planck's law at wavelength intervals of 0.1 nm. The illuminant spectrum S was normalized so that $\Sigma_{k=1}^{N} S(k)\,\bar{y}(k) = 100$, where N is the number of wavelength steps, i.e., $N = 3,001$.

To avoid switching between Type 1 and Type 2 during the optimization of $\lambda_{\text{cut-on}}$ and $\lambda_{\text{cut-off}}$, we concatenated three copies of the color-matching functions $\bar{x}_c$, $\bar{y}_c$, and $\bar{z}_c$ and the illuminant spectrum S_c. This concatenation procedure is illustrated in Fig. 3, where n is the central wavelength and h_n is the half-bandwidth of the spectral reflectance $R_n(l)$ of the optimal color on the concatenated wavelength scale l. Here, $l_{\text{cut-on}} = n - h_n$ and $l_{\text{cut-off}} = n + h_n$:

$$R_n(l) = \begin{cases} 1, & l_{\text{cut-on}} \le l \le l_{\text{cut-off}} \\ 0, & otherwise \end{cases}, \quad (1)$$

where n is an integer between $N + 1$ and $2N$, and h_n is a real number between 0 and $N/2$. It is obvious that concatenation makes it possible to treat a Type 2 band-stop reflectance as a Type 1 band-pass reflectance. Let $T_x(l)$, $T_y(l)$, and $T_z(l)$ be continuous functions obtained by linear interpolation of $S_c(l)\bar{x}_c(l)$, $S_c(l)\bar{y}_c(l)$, and $S_c(l)\bar{z}_c(l)$, respectively. The tristimulus values of the optimal color can be efficiently calculated using trapezoidal integration. The estimated tristimulus values of an optimal color were converted to the lightness value using a specified color appearance model, and this estimation was repeated in order to equalize the estimated lightness to a specified value with an accuracy of $\pm 10^{-7}$. The termination tolerance for h_n was set to 10^{-10} nm on the concatenated wavelength scale or 10^{-11} nm.
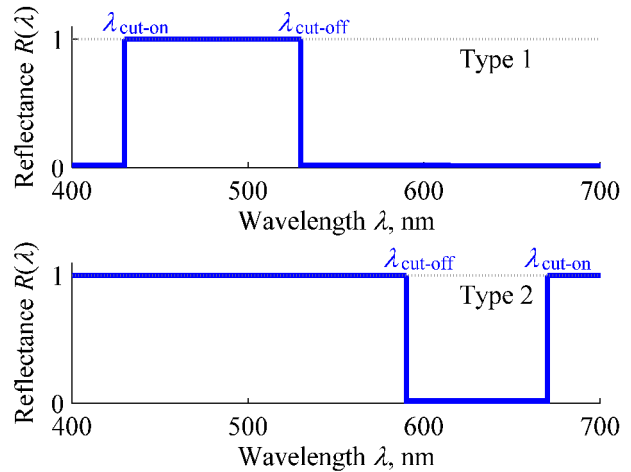
Figure 2. Two types of spectral reflectance (transmittance) for optimal colors.
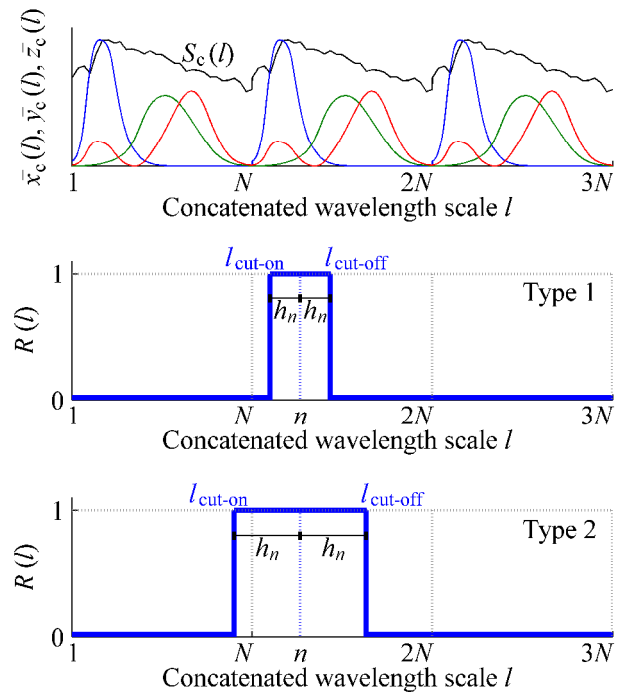
Figure 3. Concatenation of three copies of color-matching functions and illuminant spectrum (top). An optimal color has spectral reflectance R(l) with central wavelength n and half-bandwidth h_n on the concatenated wavelength scale l (center and bottom).

Color appearance model

CIELAB with von Kries-type CATs

To calculate the perceptual correlates of the optimal colors, we used CIELAB with three different chromatic adaptation transforms (CATs), CIECAM02, and CAM02-UCS. A model that contains predictors of the relative color appearance attributes lightness, chroma, and hue is referred to as a color appearance model. In that sense, CIELAB can be considered a color appearance model, although the adaptation transform is clearly less accurate than transformations that follow the known visual physiology more closely [15, 16].

To investigate how this inaccuracy affects the estimate of the number of discernible colors, we embedded some CATs based on the von Kries hypothesis [17] in the CIELAB equations. Under von Kries-type CATs, tristimulus values are linearly converted to relative cone responses and scaled so that the values of the reference white stay constant for both the destination and source conditions:

$$\begin{bmatrix} X_d \\ Y_d \\ Z_d \end{bmatrix} = \mathbf{M}^{-1} \begin{bmatrix} L_{w,d}/L_{w,s} & 0 & 0 \\ 0 & M_{w,d}/M_{w,s} & 0 \\ 0 & 0 & S_{w,d}/S_{w,s} \end{bmatrix} \mathbf{M} \begin{bmatrix} X_s \\ Y_s \\ Z_s \end{bmatrix}, \quad (2)$$

where subscripts d and s denote destination and source, respectively, and L_w, M_w, and S_w are the long-, medium-, and short-wavelength cone responses, respectively, of the reference white. The normalization in CIELAB, where the tristimulus values are normalized by those of the reference white, can be expressed by letting $\mathbf{M}$ be the 3×3 identity matrix.

We used three von Kries-type CATs: CAT02, Hunt–Pointer–Estévez (HPE), and a linearized version of the Bradford chromatic adaptation transform (BFD). CAT02 converts CIE tristimulus values to 'sharpened' cone responsivities, which are spectrally distinct and partially negative, whereas HPE fundamentals more closely represent actual cone responsivities [15]. BFD is commonly used for the profile connection space in color management. The 3×3 matrices for CAT02 ($\mathbf{M}_{CAT02}$), HPE ($\mathbf{M}_{HPE}$), and BFD ($\mathbf{M}_{BFD}$) are described as follows:

$$\mathbf{M}_{CAT02} = \begin{bmatrix} 0.7328 & 0.4296 & -0.1624 \\ -0.7036 & 1.6975 & 0.0061 \\ 0.0030 & 0.0136 & 0.9834 \end{bmatrix}, \quad (3)$$

$$\mathbf{M}_{HPE} = \begin{bmatrix} 0.38971 & 0.68898 & -0.07868 \\ -0.22981 & 1.18340 & 0.04641 \\ 0.00000 & 0.00000 & 1.00000 \end{bmatrix}, \quad (4)$$

$$\mathbf{M}_{BFD} = \begin{bmatrix} 0.8951 & 0.2664 & -0.1614 \\ -0.7502 & 1.7135 & 0.0367 \\ 0.0389 & -0.0685 & 1.0296 \end{bmatrix}. \quad (5)$$

CIECAM02 color appearance model

CIECAM02 [10] is the latest color appearance model ratified by the CIE. In our simulation, we assumed an average surround condition with three parameters ($F = 1$, $c = 0.69$, $N_c = 1.0$). The adaptation luminance L_A (in cd/m^2), which is often taken to be 20% of the luminance of the reference white, was calculated using the illuminance of the reference white in lux, E_w :

$$L_A = nE_w/\pi , \quad (6)$$

where $n = 0.2$. The source tristimulus values were converted to cone responses using the CAT02 transform matrix. Next, the cone responses were converted to adapted tristimulus responses representing the corresponding colors under an implied equal-energy illuminant reference condition. After adaptation, the cone responses were converted to the HPE responses L' , M' , and S' , which were then further modified, to prevent the calculation of a power of a negative number, as follows:

$$L'_a = \frac{L'/|L'| \cdot 400 (F_L |L'|/100)^{0.42}}{27.13 + L'/|L'| \cdot 400 (F_L |L'|/100)^{0.42}} + 0.1 , \quad (7)$$

$$M'_a = \frac{M'/|M'| \cdot 400 (F_L |M'|/100)^{0.42}}{27.13 + M'/|M'| \cdot 400 (F_L |M'|/100)^{0.42}} + 0.1 , \quad (8)$$

$$S'_a = \frac{S'/|S'| \cdot 400 (F_L |S'|/100)^{0.42}}{27.13 + S'/|S'| \cdot 400 (F_L |S'|/100)^{0.42}} + 0.1 , \quad (9)$$

where F_L is the luminance-level adaptation factor. These modifications were necessary because the bandwidth of the spectral reflectance $R(l)$ of optimal colors can be extremely narrow during optimization, producing negative responses. The lightness J, chroma C, colorfulness M, and hue h were then computed. The Cartesian coordinates for the chroma (a_C, b_C) and colorfulness (a_M, b_M) were $(C\cos(h), C\sin(h))$ and $(M\cos(h), M\sin(h))$, respectively.

CIECAM02-based uniform color space (CAM02-UCS)

CIECAM02 does not necessarily assume a color space that is perceptually uniform in terms of color differences. To allow a uniform color space to be used, Luo et al. [12] made the following modifications to the CIECAM02 lightness and colorfulness:

$$J' = 1.7J/(1 + 0.007J) , \quad (10)$$

$$M' = (1/0.0228)\ln(1 + 0.0228M) . \quad (11)$$

The Cartesian coordinates (a', b') are $(M'\cos(h), M'\sin(h))$.

Estimation of the number of discernible colors

The number of discernible colors can be estimated by counting the just-noticeable difference (JND) unit cells within a color solid. In the simple, popular square-packing method, the number of JND unit squares packed in each locus embodying a solid is counted [7, 9]. Estimates based on this method fluctuate, however, depending on the sampling sites. Rather, the volume can be used to approximate the number of discernible colors without such ambiguities if each locus contains many color-difference unit squares.

We calculated the volume of optimal color solids in the CIELAB (L^*, a^*, b^*) , CIECAM02 (J, a_C, b_C) and (J, a_M, b_M) , and CAM02-UCS (J', a', b') color spaces. First, 100 optimal color loci were obtained at lightness values from 0.5 to 99.5, at intervals of 1 for each color space. Each locus consisted of 3,001 optimal colors with central wavelengths between 400 nm and 700 nm at 0.1 nm intervals. The approximate volume of each color solid was obtained by summing the areas of the loci. The area of

each convex or concave locus specified by the N vertices of (a_k, b_k), $k = 1, 2, …, N$, was calculated by the shoelace algorithm, which can compute the area of a simple polygon whose vertices are described by ordered pairs in the plane as $\left|\Sigma_{k=1}^{N}(a_k b_{k+1} - a_{k+1} b_k)\right|/2$, where $a_{N+1} = a_1$ and $b_{N+1} = b_1$.

We also computed the number of CIE94 color differences ($S_L = 1$, $k_1 = 0.045$, $k_2 = 0.015$, $k_L = k_C = k_H = 1$) within the color solid in the CIELAB color space. This can be estimated by slicing the solid at regular intervals over the lightness range. For simplicity, we denote $\Delta C_{94}^* = \Delta C_{ab}^*/S_C$ and $\Delta H_{94}^* = \Delta H_{ab}^*/S_H$. If the two colors have a constant lightness value and hue, then:

$$\Delta C_{94}^* = \frac{\Delta C_{ab}^*}{1 + k_1\sqrt{(C_{ab1}^* + \Delta C_{ab}^*)C_{ab1}^*}} . \quad (12)$$

By taking the limit of Eq. (12), we derive a differential equation for the chroma:

$$\frac{dC_{94}^*}{dC_{ab}^*} = \lim_{\Delta C_{ab}^* \to 0} \frac{\Delta C_{94}^*}{\Delta C_{ab}^*} = \frac{1}{1 + k_1 C_{ab}^*} . \quad (13)$$

Next, consider that the two colors have a constant chroma of $C_{ab}^*/\cos(\Delta h_{ab}/2)$, at the middle point of which is C_{ab}^*, and a constant lightness value. When $|\Delta h_{ab}| \ll 1$:

$$\Delta H_{ab}^* = 2C_{ab}^* \tan(\Delta h_{ab}/2) \approx C_{ab}^* \Delta h_{ab} . \quad (14)$$

In this case, ΔH_{94}^* can be approximated as:

$$\Delta H_{94}^* \approx \frac{C_{ab}^* \Delta h_{ab}}{1 + k_2 C_{ab}^*} . \quad (15)$$

Consider an isosceles triangle whose base is ΔH_{94}^* and height is C_{ab}^*; when the apex of the triangle is positioned at the achromatic point ($a^* = b^* = 0$), the number of CIE94 color differences ΔA_{94}^* within the triangle is approximately:

$$\begin{aligned}
\Delta A_{94}^* &= \int_0^{C_{ab}^*} \Delta H_{94}^* dC_{94}^* \approx \int_0^{C_{ab}^*} \frac{C_{ab}^* \Delta h_{ab}^*}{1 + k_2 C_{ab}^*} \frac{dC_{ab}^*}{1 + k_1 C_{ab}^*} \\
&= \Delta h_{ab}^* \cdot \frac{k_1 \ln(k_2 C_{ab}^* + 1) - k_2 \ln(k_1 C_{ab}^* + 1)}{k_1 k_2 (k_1 - k_2)} .
\end{aligned} \quad (16)$$

Given that the nth optimal color of N points enclosing a two-dimensional area has a hue difference of $\Delta h_{ab}(n)$ and chroma $C_{ab}^*(n)$, $\Delta h_{ab}(n) = (h_{ab}(n-1) - h_{ab}(n+1))/2$. Note that $\Delta h_{ab}(n)$ may be negative. The number of CIE94 color differences in the area enclosed by a locus consisting of N optimal colors is calculated as $\Sigma_{n=1}^{N} \Delta A_{94}^*(n)$, where $h_{ab}(0) = h_{ab}(N)$ and $h_{ab}(N+1) = h_{ab}(1)$. The total number of CIE94 color differences within an optimal color solid is then calculated by summing the number of CIE94 color differences of the 100 loci obtained in the CIELAB color space.

Results

Figure 4 shows the volume of optimal color solids in the CIELAB unit cube (top) and the number of CIE94 color differences (bottom) as a function of the CCT of the light sources, which consisted of blackbody radiators (2,000–4,000 K) and daylight illuminants (4,000–10,000 K). The volumes were calculated with and without the von Kries-type CATs embedded in front of CIELAB. The results clearly show that the number of discernible colors and the variation with the CCT of the adaptation light source depend on the color model used. The breaks in the curves at 4,000 K are due to the switch from the spectral power

distribution of the blackbody radiator to that of the daylight illuminant. The estimated number of colors at a CCT of 6,500 K is 2,286,919 in the CIELAB unit cube, which is close to Pointer and Attridge's [7] estimate of 2.28 million, and the number of CIE94 color differences is 351,791, which is close to Wen's [8] estimate of 352,263. Considering that one JND corresponds to half of the CIE94 unit, the estimate for the number of discernible colors should be larger than the number of CIE94 color differences by a factor of eight. At 6,500 K, the volume is estimated to be 2,110,746, which is again close to Pointer and Attridge's estimate.

Figure 5 shows the volume of optimal color solids in the CIECAM02 (J, a_C, b_C) and (J, a_M, b_M) spaces as a function of the CCT for E_w of 200 lx, 1,000 lx, 10,000 lx, and 100,000 lx. Morovic et al.'s [11] estimate of 3.8 million under illuminant D50 with E_w of approximately 1,000 lx is considerably larger than our estimate of 2,078,589. In addition, their estimate of 4.2 million under illuminant F11 seems especially large. Figure 6 shows the results of Martínes-Verdú et al. [9] and our estimate for an E_w value of 1,571 lx ($L_A = 100$). These results are similar, although their highest estimate under illuminant E does not match ours. Figure 7 shows the volume of optimal color solids in the CAM02-UCS (J', a', b') space. The volume increases with the CCT and illuminance of the reference white, which is the same trend as in Fig. 5 (bottom), although the estimate is much smaller than the others.
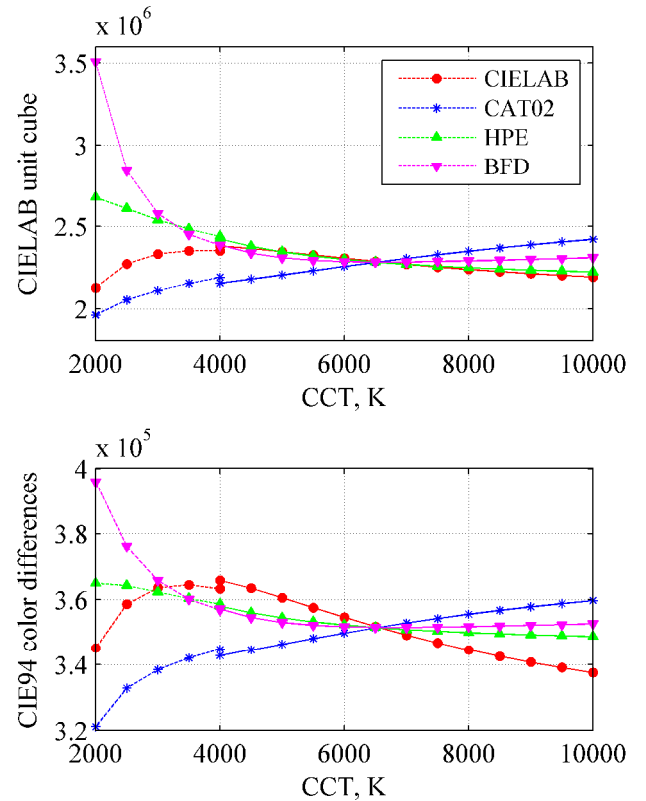
Figure 4. Volume of optimal color solids in CIELAB unit cube (top) and the number of CIE94 color differences (bottom) calculated with and without von Kries-type CATs (CAT02, HPE, and BFD) embedded in front of CIELAB as a function of the CCT of the light sources (dotted lines: blackbody radiator, solid lines: daylight illuminant).

Discussion

As shown in Fig. 4, the volume estimated using CIELAB (without the von Kries-type CATs) peaks at around 4,000 K. The estimates made using CAT02 increase with the CCT, whereas those made using HPE and BFD decrease. The CIECAM02 (Fig. 5) and CAM02-UCS (Fig. 7) estimates increase as the CCT increases, which is reasonable because the CAT02 chromatic adaptation transform was the main part of CIECAM02. The matrix coefficients of CAT02 in Eq. (3) and BFD in Eq. (5) are relatively close to each other, whereas the shapes of the curves differ, indicating that a slight difference in the coefficients of the CAT matrices produces different trends in volume estimation.

It might be suitable to use CAM02-UCS rather than CIECAM02 for the estimation, because CIECAM02 was originally designed as a color appearance model, not a uniform color space in terms of color differences. The CIECAM02 lightness–colorfulness space was selected as the base color space of CAM02-UCS because its performance factor measure (PF/3) was slightly better in the lightness–colorfulness space than in the lightness–chroma space [18]. The significant dependence of the volume estimation on the adaptation luminance level was not taken into account. Moreover, the combination of lightness and colorfulness might be unreasonable, because lightness is a relative color appearance attribute whereas colorfulness is an absolute one [15]. It seems to be natural in terms of matching the scale type to use brightness–colorfulness or lightness–chroma, although further study is needed to determine which color space is reasonable for computing the volume of color solids.

Martínes-Verdú *et al*. [9] suggested the possibility of an alternative color-rendering index based on the number of discernible colors within an optimal color solid. As shown in Fig. 6, however, their highest number under illuminant E did not match ours, which is due to miscalculation on their part. Morovic *et al*. [11] showed a relationship between CCT and gamut volume in CIECAM02, with higher CCT giving rise to a greater number of colors. Although this trend corresponds to our results, it is simply an artifact of CAT02.
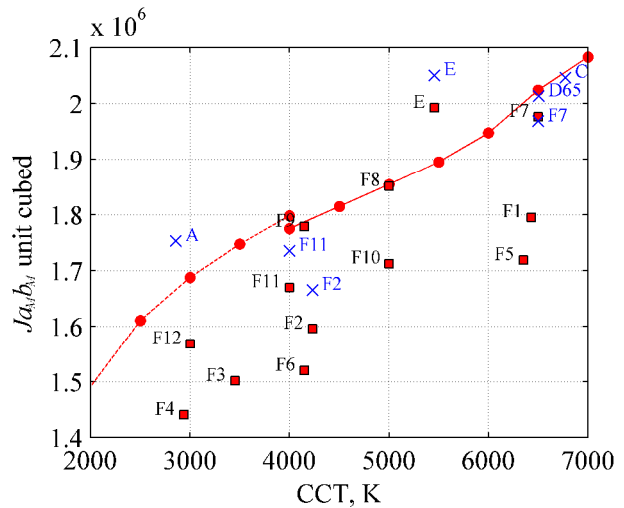
Figure 6. Volume of optimal color solids in the CIECAM02 lightness–colorfulness space as a function of the CCT of the light sources with the illuminance of the reference white of 1,571 lx (dotted lines: blackbody radiator, solid lines: daylight illuminant, squares: illuminant series F and illuminant E, crosses: Estimate of Martínes-Verdú et al. [9]).

Figure 5. Volume of optimal color solids in the CIECAM02 lightness–chroma (top) and lightness–colorfulness (bottom) spaces as a function of the CCT of the light sources with the illuminance of the reference white of 200 lx, 1,000 lx, 10,000 lx, and 100,000 lx (dotted lines: blackbody radiator, solid lines: daylight illuminant).
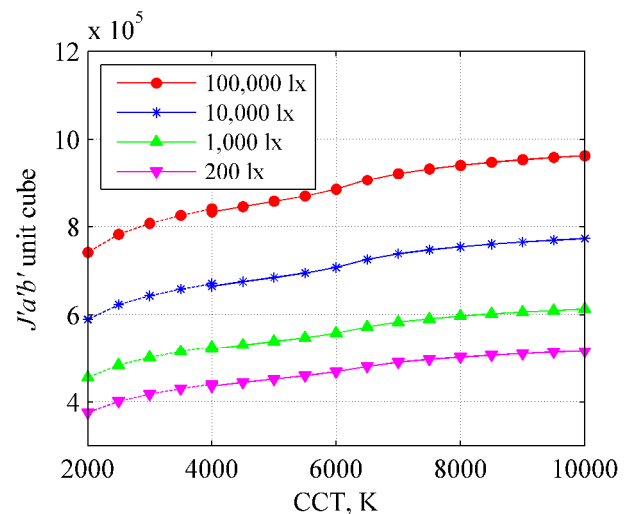
Figure 7. Volume of optimal color solids in the CAM02-UCS space as a function of the CCT of the light sources with the illuminance of the reference white of 200 lx, 1,000 lx, 10,000 lx, and 100,000 lx (dotted lines: blackbody radiator, solid lines: daylight illuminant).
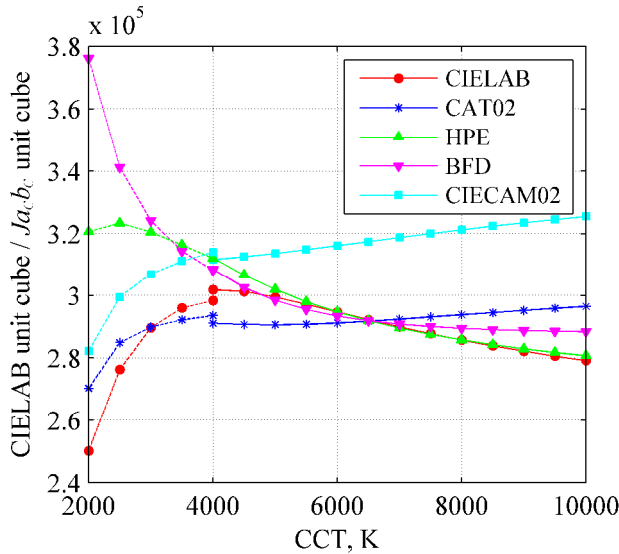
Figure 8. Volume of Munsell matte colors in the CIELAB unit cube calculated with and without von Kries-type CATs (CAT02, HPE, and BFD) and in the CIECAM02 lightness-chroma space (1,000 lx) as a function of the CCT (dotted lines: blackbody radiator, solid lines: daylight illuminant).

Morovic *et al*. [11] noted that any color appearance model fails to estimate the number of discernible colors within an optimal color solid because the gamut is larger than the psychophysical data it is derived from. In addition, CIELAB was optimized on the basis of the Munsell system, which is defined only for the CIE 1931 standard observer and illuminant C [19]. Therefore, we estimated the number of discernible colors within a small color gamut using a dataset [20] consisting of the reflectance spectra of 1,269 color chips in the matte edition of the Munsell Book of Color. Figure 8 shows the volume of the convex hull in the CIELAB unit cube and the CIECAM02 (J, a_C, b_C) unit cube, as a function of the CCT of the light sources when the illuminance of the reference white was 1,000 lx. However, the variations in volume again depend on the CAT.

To elicit the unknown, we must find a non-von Kries-type CAT or a completely new color appearance model, but that is well beyond the scope of this paper, or indeed any single paper. Although our research shows negative results, we believe it is a significant step in the advancement of color science.

Conclusions

We estimated the number of discernible colors over a wide range of color temperatures and illuminance levels using several chromatic adaptation models, color spaces, and limens of color differences. Through this comprehensive simulation, it was found that the estimates are highly dependent on the color model used. The variations in volume as a function of color temperature were mainly determined by the CAT, and slight differences in the coefficients of the CAT matrices caused different trends in the estimation. As far as the ranking of the number of discernible colors is concerned, it is premature to compare the estimates at different color temperatures and illuminance levels. Thus, the number of discernible object colors remains unknown.

References

[1] J. Morovic, P. L. Sun, and P. Morovic, "The gamuts of input and output colour imaging media," Proc. SPIE 4300, pp. 114–125, 2000.
[2] R. G. Kuehni, *Color Space and its Divisions: Color Order from Antiquity to the Present* (Wiley, 2003), pp. 202–203.
[3] W. Ostwald, "Neue Forschungen zur Farbenlehre," Phys. Z. 17, pp. 322–332, 1916.
[4] E. Schrödinger, "Theorie der Pigmente von grösster Leuchtkraft," Ann. Phys. 62, pp. 603–622, 1920.
[5] D. L. MacAdam, "The theory of maximum visual efficiency of colored materials," J. Opt. Soc. Am. 25, pp. 249–252, 1935.
[6] D. L. MacAdam, "Maximum visual efficiency of colored materials," J. Opt. Soc. Am. 25, pp. 361–367, 1935.
[7] M. R. Pointer and G. G. Attridge, "The number of discernible colors," Col. Res. Appl. 23, pp. 52–54, 1998.
[8] S. Wen, "A method for selecting display primaries to match a target color gamut," J. Soc. Inf. Disp. 15, pp. 1015–1022, 2007.
[9] F. Martínes-Verdú, E. Perales, E. Chorro, D. de Fez, and V. Viqueira, "Computation and visualization of the MacAdam limits for any lightness, hue angle, and light source," J. Opt. Soc. Am. A 24, pp. 1501–1515, 2007.
[10] CIE, CIE TC8-01 Technical Report, *A Colour Appearance Model for Color Management Systems*: CIECAM02, CIE Pub. 159 (2004).
[11] J. Morovic, V. Cheung, and P. Morovic, "Why we don't know how many colors there are," Proc. IS&T CGIV 2012: Sixth European Conference on Colour in Graphics, Imaging, and Vision, pp. 49–53, 2012.
[12] M. R. Luo, G. Cui, and C. Li, "Uniform colour spaces based on CIECAM02 colour appearance model," Col. Res. Appl. 31, pp. 320–330, 2006.
[13] K. Masaoka, "Fast and accurate model for optimal color computation," Opt. Lett. 35, pp. 2031–2033, 2010.
[14] G. Wyszecki and W. S. Stiles, *Color Science: Concepts and Methods, Quantitative Data and Formulae* (Wiley, 2000).
[15] M. D. Fairchild, *Color Appearance Models*, 2nd ed. (Wiley, 2005).
[16] M. D. Fairchild, "Testing colour-appearance models: Guidelines for coordinated research," Col. Res. Appl. 20, pp. 262–267, 1995.
[17] J. von Kries, "Chromatic Adaptation," Festschrift der Albercht-Ludwig-Universität, 1902.
[18] C. Li, M. R. Luo, and G. Cui, "Colour-differences evaluation using colour appearance models," Proc. IS&T/SID CIC11: Eleventh Color Imaging Conference, pp. 127–131, 2003.
[19] S. M. Newhall, D. Nickerson, and D. B. Judd, "Final report of the O.S.A. subcommittee on the spacing of the Munsell colors," J. Opt. Soc. Am. 33, pp. 385–418, 1943.
[20] University of Eastern Finland, *Spectral Image Database*, http://spectral.joensuu.fi/.

Author Biography

Kenichiro Masaoka received his B.S. (1994), M.S. (1996), and Ph.D. (2009) degrees in electronic engineering, energy engineering, and engineering from the Tokyo Institute of Technology, Japan, respectively. He is currently a principal research engineer at NHK Science and Technology Research Laboratories, Tokyo, and is involved in developing ultrahigh definition television. He is a member of the IEEE and Institute of Image Information and Television Engineers of Japan.